Available online at www.sciencedirect.com
SCIENCE DIRECT®
ELSEVIER
Journal of Nuclear Materials 322 (2003) 249–254
journal of nuclear materials
www.elsevier.com/locate/jnucmat

Fracture surface topography analysis of in-beam fatigue behavior for 20% cold-worked 316 stainless steel

Y. Murase [a,*], Johsei Nagakawa [a,b], N. Yamamoto [a]

[a] *Materials Engineering Laboratory, Materials Reliability Group, National Institute for Materials Science (NIMS), 1-2-1 Sengen, Tsukuba, Ibaraki 305-0047, Japan*

[b] *Interdisciplinary Graduate School of Engineering Sciences, Kyushu University, 6-1 Kasuga Koen, Kasuga, Fukuoka 816-8580, Japan*

Received 25 November 2002; accepted 23 August 2003

Abstract

Topography on the fatigue fracture surface was examined by using a confocal laser microscope for the side-notched small specimens of 20% cold-worked 316 stainless steel fractured in stress-controlled fatigue tests under the in-beam (dynamic), post-irradiation (static) and unirradiation conditions with 17 MeV protons at 60 °C. A technique of the fracture surface topography analysis (FRASTA) was adopted to extract the information of plastic deformation at the crack tip for the in-beam, post-irradiation and unirradiated specimens. The progress in plastic deformation at the crack tip was significantly delayed in the dynamic irradiation condition while not so much as in the static irradiation condition. The present results of FRASTA would not only support the superiority of dynamic irradiation effect to the static irradiation effect on fatigue behavior but also provide good evidence for the mechanism of the dynamic irradiation effect based on the interaction between continuously induced defect clusters and mobile dislocations.

1. Introduction

Fusion reactor materials will be subjected to severe atomic displacement damage and external loadings such as thermal and magnetic stresses, simultaneously. Since the external loadings include cyclic component in their nature due to periodic operation of fusion reactor, it is important to understand the in-beam fatigue behavior of structural materials in order to construct the material design concept of fusion reactor. In the course of increasing demand on the understanding of in-beam fatigue behavior during the recent decades, some workers [1–3] have reported some essential differences in the fatigue behavior of type 316 stainless steel between in-beam (dynamic) and post-irradiation (static) conditions; the lifetime in the in-beam fatigue tests is longer than that in the post-irradiation tests. In the previous study [1], Murase et al. have conducted the stress-controlled fatigue tests for the single side-notched small specimens of 20% cold-worked 316 stainless steel under the in-situ (dynamic), post-irradiation (static) and unirradiation conditions with 17 MeV protons at 60 °C. The fatigue life was substantially prolonged in the in-situ irradiation condition, whereas a slight increase of lifetime was detected in the post-irradiation condition. Fatigue striations on the fracture surface has been also examined by a scanning electron microscope (SEM) for all specimens. The striation analysis suggested that substantial extension of fatigue lifetime in the in-situ irradiation condition was mainly attributed to the delay in the processes of crack initiation and growth until 100 μm in length. Although the higher resistance to fatigue fracture in the dynamic irradiation condition has been demonstrated from SEM measurement on fracture surface, any direct evidence for the mechanism of the dynamic irradiation effect on fatigue behavior could not be obtained in the previous work.

* Corresponding author. Tel.: +81-29 859 2014; fax: +81-29 859 2014/2552.
E-mail address: murase.yoshiahru@nims.go.jp (Y. Murase).

0022-3115/$ - see front matter © 2003 Elsevier B.V. All rights reserved.
doi:10.1016/j.jnucmat.2003.08.027

A new fractographic technique, fracture surface topography analysis (FRASTA), has been developed to reconstruct fracture events in microscopic details by qualifying and analyzing the topographies of conjugate surfaces simultaneously [4]. The technique can provide some indications of fracture toughness, crack initiation site, crack growth rate, the crack-opening displacement and plastic deformation at the crack tip. In particular, the information of plastic deformation at the crack tip is inaccessible from SEM measurement, hence it could offer a new way to evaluate how the higher resistance to fatigue fracture is produced in the dynamic irradiation condition. In the present study, three-dimensional topographic data on the conjugate fracture surfaces were measured by using a laser confocal microscope for the in-beam, post-irradiation and unirradiated specimens. The objective of the present work is to improve the understanding of the dynamic irradiation effect on fatigue behavior by means of FRASTA technique.

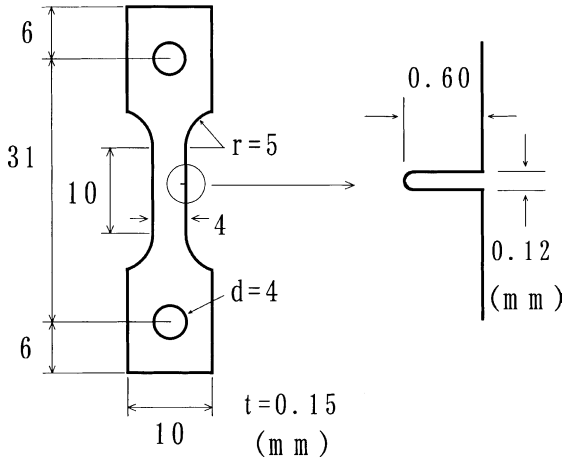

Fig. 1. Dimensions of the single side-notched specimen for fatigue tests.

2. Experimental procedure

In the previous study [1], fatigue tests had been conducted for 20% cold-worked 316 stainless steel under in-beam, post-irradiation and unirradiation conditions with 17 MeV protons at 60 °C. Chemical composition of the steel and dimensions of the single side-notched fatigue specimen are shown in Table 1 and Fig. 1, respectively. Cyclic loading mode was triangular wave in stress control with the maximum stress of 536.4 MPa and the minimum stress of 236.4 MPa under a constant loading rate of 50 MPa/s. In the present 17 MeV proton irradiation, atomic displacement rate was adjusted to 1×10^{-7} dPa/s with an error range of ±11%. The details of specimen preparation, irradiation condition and the in-beam fatigue experimental machine were described elsewhere [5]. The specimens fractured in the previous fatigue tests were used for the present study. The three-dimensional topographic data on the conjugate fracture surfaces were obtained by using a blue laser confocal microscope (Lasertec.VL2000) for the in-beam, post-irradiation and unirradiated specimens. The resolution of the topographic data was 0.36 μm/pixel and 0.59 μm/scan in XY plane and depth (Z direction), respectively. The topographic maps of the conjugate fracture surfaces were stored in a computer, and one fracture surface was inverted to superimpose on the other map of the coupled surface. The analytical procedures of FRASTA technique [6] are shown in Figs. 2(a)–(d) with schematic illustrations of cross-sectional plots (XSPs). The coordinates of the two maps were adjusted precisely to coincide the corresponding configurations such as ratchet-marks and dimples on the conjugate surfaces (Fig. 2(a)). Then the inclination angle θ was introduced to 3D data of the conjugate surfaces along the direction of crack propagation in order to compensate the elastic deformation at the crack tip (Fig. 2(b)). In the present study, the angle of θ was deliberately selected as 3.5° so that (1) the shape of main crack front was consistent with the configurations on the fracture surface and (2) micro-cracks ahead of main crack front did not come back to the front during the analysis [6]. When two maps were set together at the notch tip (Fig. 2(c)), then one of the maps was detached gradually (Fig. 2(d)). The fractured area projection plots (FAPPs) were also presented in Figs. 2(c) and (d). In these plots, un-overlapped areas (fractured areas) are indicated as white and overlapped areas (un-fractured areas) are dark. Fig. 3 shows a typical series of FAPPs for the unirradiated specimen with increasing opening of the conjugate surfaces (denoted as d). In FAPPs, the distance of main-crack front from the notch tip (denoted as l) is calculated as

$$l = l_{\mathrm{all}} \times A/A_{\mathrm{all}},$$

where A is the fractured area, A_{all} is the total area of the projection plots and l_{all} is the length of the plots in the

Table 1
Chemical compositions of 316 stainless steel (wt%)

C	Ni	Cr	Mn	Mo	Si	P	S	Fe
0.06	10.30	16.79	1.17	2.16	0.68	0.027	0.001	Balance

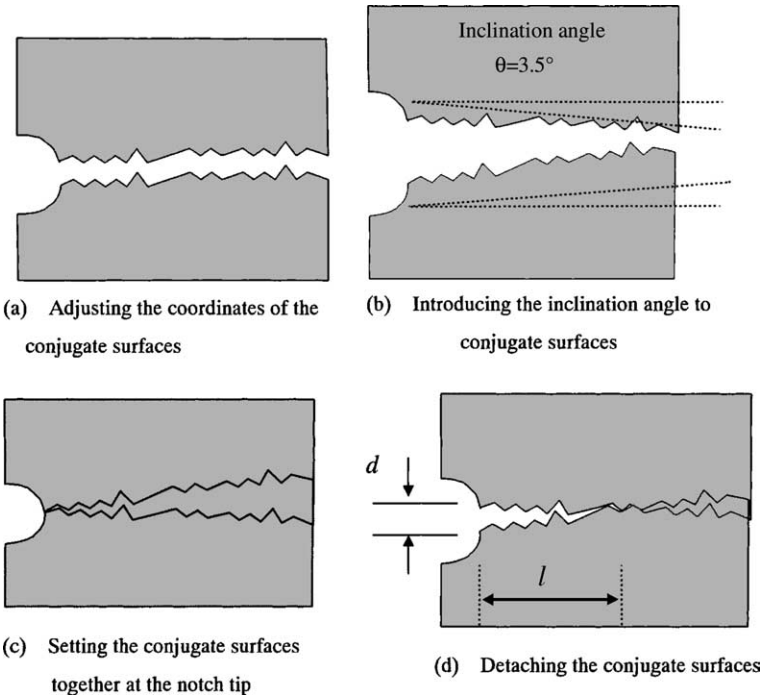

Fig. 2. Analytical procedure of FRASTA.

direction of crack propagation at $d = 0$ [7]. The opening of the conjugate surfaces, d, was plotted with the distance of main-crack front from the notch tip, l, for all specimens. In this plotting of d with l, the slope of plotting $(\Delta d/\Delta l)_N$ at Nth plot (l_N, d_N) is roughly calculated as

$$(\Delta d/\Delta l)_N = (d_{N+1} - d_{N-1})/(l_{N+1} - l_{N-1}) \quad (N \geqslant 1),$$

where the initial plot $(l_0, d_0) = (0, 0)$. The slope of plotting, $\Delta d/\Delta l$, was also plotted with l for all specimens.

3. Results

Fig. 4 presents the plotting of (a) d and (b) $\Delta d/\Delta l$ with l for all specimens. The additional dashed line of $d = 2l \times \tan 3.5°$ shown in Fig. 4(a) stands for the increment of d accompanied with the inclination angle of $\theta = 3.5°$. The plots were considerably fitted on the dashed line until about 400 μm for all specimens, and substantial deviation from the dashed line started around 450 μm for the post-irradiation and unirradiated specimens. Although the plotting was quite similar for the post-irradiation and unirradiated specimens, considerable fit of plots on the dashed line was further extended until about 700 μm for the in-beam specimens. As for the plotting of $\Delta d/\Delta l$ with l shown in Fig. 4(b), the plots were fairly fitted on the dashed line of $\Delta d/\Delta l = 2 \times \tan 3.5°$ within the scattering range of $2 \times \tan 3.5° \pm 70\%$ until about 400 μm for all specimens. When a point where $\Delta d/\Delta l$ changes beyond the scattering range is designated as the bending point in this paper, the bending point seemed to be around 450 μm for the post-irradiation and unirradiated specimens and around 700 μm for the in-beam specimens, as shown in Fig. 4(a) and (b).

Striation analysis on the fracture surface has been conducted for the in-beam, post-irradiation and unirradiated specimens in the previous study [1]. Fig. 5 shows the variation of striation spacing with the distance from the notch tip for all specimens. Since the striation spacing has been considered to agree with crack growth per one cycle when it is in the range from 0.1 to 1.0 μm [8], one-to-one correlation between fatigue cycle and striation spacing is applicable to the results of striation analysis shown in Fig. 5. In comparison of results between the FRASTA (Fig. 4(a)) and the striation analysis (Fig. 5), the bending point appeared to be in good agreement with the beginning of rapid increase in striation spacing for all specimens. Striation spacing was smaller until 500 μm for the post-irradiation specimen than that for unirradiated specimens (see Fig. 5), irrespective of quite similar plotting for both specimens (see Fig. 4(a)).

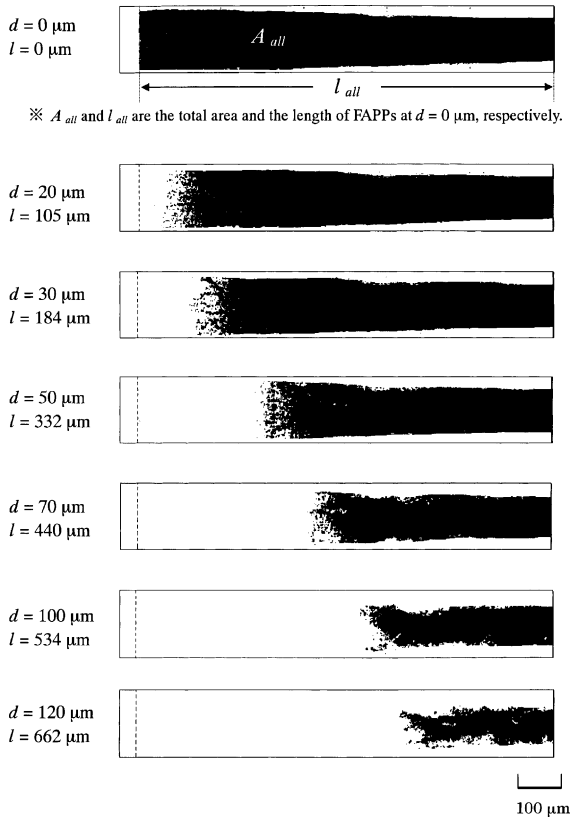

Fig. 3. Typical series of FAPPs for the unirradiated specimen.

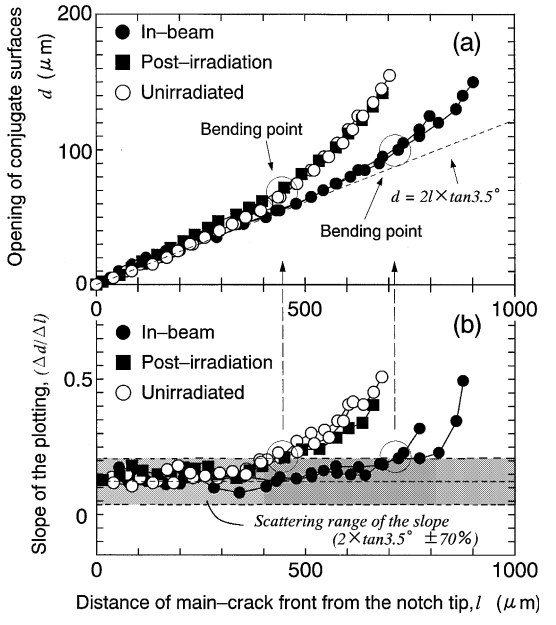

Fig. 4. The plotting of (a) d and (b) $\Delta d/\Delta l$ with l for all specimens.

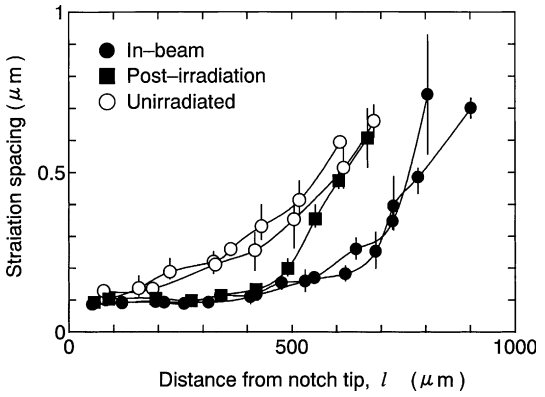

Fig. 5. The variation of striation spacing with increasing distance from notch tip.

4. Discussion

4.1. Comparison of results between FRASTA and striation analysis

The relation of the progressing main-crack front with the opening of the conjugate fracture surfaces, namely the plotting of l with d shown in Fig. 4(a), is well known as a fracture progression curve (FPC) [9]. The FPC can be utilized to estimate not only the crack tip opening displacement (CTOD) related to the J-integral or stress intensity factor [7] but also the locations of overloads or environmental changes during the fracture tests [9,10]. Kobayashi and co-workers have adopted FRASTA technique to deduce crack growth rate of vessel tube by addressing the changes in slope of FPC on the loading and temperature histories [10]. Even in the isothermal fatigue tests under constant fatigue loading condition, the rapid increase in the slope of FPC would reflect the transition of fatigue cracking mode (from Stage II_b to II_c) [11] followed by large-scale plastic deformation at the crack tip before the ductile fracture. In the present results of FRASTA shown in Fig. 4(a), therefore, the deviation of the plots from the dashed line indicates the progress in plastic deformation at the crack tip during the process of crack propagation. The comparison of results between FRASTA (Fig. 4(a)) and striation analysis (Fig. 5) revealed good agreement between the bending point and the beginning of rapid increase in striation spacing for all specimens. Since striation spacing corresponds to crack growth rate in this case, it is reasonably suggested that the development of large-scale plastic deformation at the crack tip could be correlated with rapid increase of crack growth rate. The progress in plastic deformation at the crack tip could be also estimated with the number of fatigue cycles for each specimen. Smaller striation spacing with further extended cracking area until about 700 μm in the in-beam specimens implies the larger number

of fatigue cycles to the development of large-scale plastic deformation in the dynamic irradiation condition. Even in the post-irradiation specimen, smaller striation spacing until about 500 μm indicates slight increase in the number of cycles to the substantial plastic deformation in the static irradiation condition. Therefore, the progress in plastic deformation at the crack tip would be significantly delayed in the dynamic irradiation condition while not so much in the static condition.

4.2. The effect of in-situ irradiation on crack propagation

It is well known that fatigue behaviors are closely associated with the rearrangement of dislocation structures. Some workers have reported the evolution of inhomogeneous dislocation structures such as cells and wall-channels at the plastic deformed zone in the vicinity of crack tip for type 316 stainless steels [12,13]. The formation of the inhomogeneous dislocation structures plays an important role in accommodating the plastic strain accumulated during cyclic loading [14]. The saturation of the inhomogeneous dislocation structures results in the emergence of planer slip leading to the initiation and growth of fatigue cracks [14]. This consecutive rearrangement of dislocation structures would be modified by the introduction of the radiation-induced defects (RID) clusters. The general assumption is that the RID clusters act as obstacles against the dislocation glide, thereby enhancing the resistance to the evolution of inhomogeneous dislocation structures. In the meanwhile, however, the RID clusters could be absorbed or swept away during dislocation glides on the planar slips when the RID clusters are unstable against the interaction with mobile dislocations. Since the RID clusters are continuously induced into the materials in the dynamic irradiation condition, the in-beam fatigue behavior is expected to be essentially different from that in the static condition where the defect clusters are already induced prior to the fatigue test. In the previous study [1], substantial prolongation of fatigue life was reported for 20% cold-worked 316 stainless steel in the in-situ irradiation condition with 17 MeV protons at 60 °C while fatigue life slightly increased in the post-irradiation condition. The explanation of the superiority of dynamic irradiation effect to static effect on fatigue behavior at 60 °C has been attempted on the basis of the interaction between RID clusters and mobile dislocations. In the post-irradiation, a number of RID clusters are implanted into the material prior to the fatigue cycling. The density of the pre-implanted RID clusters would be reduced at the crack tip where the plastic deformation is accumulated during fatigue cycling, because the RID clusters could not grow enough to be stable against mobile dislocations at 60 °C. Since numerous fatigue cycles are necessary to initiate cracks through the rearrangement of dislocation structure, an extensive decrease in density of RID clusters would lead to little impact of static irradiation effect on the process of crack initiation. Although the pre-implanted RID clusters could survive and act as the temporary obstacles against dislocation glides when the crack propagates with less numerous cycles involved at the crack tip, this temporary interaction would not be dominant enough to extend the cracking area of the post-irradiation specimen further than those of the unirradiated specimens (see Fig. 5). Therefore, smaller striation spacing until 500 μm for the post-irradiation specimen shown in Fig. 5 may reflect the interaction between the pre-implanted RID clusters and mobile dislocations. In contrast, the RID clusters are continuously induced into the plastic deformed zone at the crack tip in the dynamic irradiation condition. The balance between continuous introduction and annihilation of RID clusters would keep the higher density of RID clusters and provide the persistent obstacles against dislocation glides at the deformed zone. Since the development of inhomogeneous dislocation structures would be persistently delayed during the in-beam fatigue tests, the dynamic irradiation effect should have substantial influence on not only the process of crack initiation but also the process of crack propagation. The interaction between continuously induced RID clusters and mobile dislocations may be responsible for smaller striation spacing with the further extended cracking area for the in-beam specimens (see Fig. 5). However in the previous study, these interpretations of the dynamic/static irradiation effects were based on the general assumption, so that some quantitative evidences have been definitely needed to demonstrate them.

In the present study, significant delay of the progress in plastic deformation at the crack tip was suggested in the in-beam specimen while not so much in the post-irradiation specimen. Since the plastic deformation involves the evolution of inhomogeneous dislocation structures, the higher resistance to the development of inhomogeneous dislocation structures would be strongly indicated in the dynamic irradiation condition. Therefore, the present results of FRASTA may not only support the superiority of dynamic irradiation effect to the static irradiation effect on fatigue behavior but also provide good evidence for the mechanism of the dynamic irradiation effect based on the interaction between continuously induced RID clusters and mobile dislocations. Thus, a technique of FRASTA is a powerful tool to evaluate the material fatigue behavior, and it could be the alternative to the striation analysis even in some ferritic stainless steels where no fatigue striation is detectable due to the intrinsic rough morphology on the fracture surface.

5. Conclusions

The FRASTA was applied to examine the fatigue behavior of 20% cold-worked 316 stainless steel fractured in

the stress-controlled tests under the in-beam (dynamic), post-irradiation (static) and unirradiation conditions with 17 MeV protons at 60 °C. The information of plastic deformation at the crack tip was extracted by means of a technique of FRASTA for all specimens. The comparison of results between FRASTA and the striation analysis indicated that the development of substantial plastic deformation at the crack tip could be correlated with rapid increase in crack growth rate. It is suggested that the progress in plastic deformation was significantly delayed in the dynamic irradiation condition while not so much in the static condition. The results of FRASTA would not only support the superiority of dynamic irradiation effect to the static irradiation effect on fatigue behavior but also provide good evidence for the mechanism of the dynamic irradiation effect based on the interaction between continuously induced defect clusters and mobile dislocations. The usefulness of FRASTA in understanding the in-beam fatigue behavior was demonstrated in the present paper.

Acknowledgements

This work was financially supported by the Budget for Nuclear Research of the Ministry of Education, Culture, Sports, Science and Technology, based on the screening and counseling by the Atomic Energy Commission.

References

[1] Y. Murase, J. Nagakawa, N. Yamamoto, J. Nucl. Mater. 302 (2002) 211.
[2] R. Scholz, J. Nucl. Mater. 212–215 (1994) 546.
[3] H. Mizubayashi, S. Okuda, K. Nakagome, H. Shibuki, S. Seki, Mater. Trans. Jpn. Inst. Metals 25 (1984) 257.
[4] T. Kobayashi, D.A. Shockey, Adv. Mater. Proc. 140 (5) (1991) 28.
[5] Y. Murase, J. Nagakawa, N. Yamamoto, Y. Fukuzawa, ASTM STP 1366, ASTM, West Conshohocken, 2000, p. 713.
[6] M. Fujiwara, T. Hattori, J. Soc. Mater. Sci., Jpn. 47 (10) (1998) 1088.
[7] N. Otsuka, T. Kobayashi, K. Watashi, M. Kikuchi, Eng. Fract. Mech. 49 (6) (1994) 859.
[8] T. Yokobori, T. Aizawa, J. Jpn. Inst. Metals 39 (1975) 1003.
[9] T. Kobayashi, D.A. Shockey, G. Ogundele, D.D. McNabb, D. Sidey, J. Test. Eval. JTEVA 22 (4) (1994) 309.
[10] T. Kobayashi, D.A. Shockey, C.G. Schmidt, R.W. Klopp, Int. J. Fatigue 19 (Suppl. 1) (1997) S237–S244.
[11] P.J. Forsyth, Acta Metall. 11 (1963) 703.
[12] W.-Y. Maeng, M.-H. Kim, J. Nucl. Mater. 282 (2000) 32.
[13] S.N. Ghafouri, R.G. Faulkner, T.E. Chung, Mater. Sci. Technol. 2 (1986) 1223.
[14] M. Gerland, J. Mendez, P. Violan, B. Ait Saadi, Mater. Sci. Eng. A 118 (1989) 83.